AVO and Seismic Processing Implications from a Regional Database of Velocity and Other Acoustic Rock Property Trends

H.R. Nelson, Jr. (Geophysical Development Corp.),*
S.D. LeRoy (EarthView Associates, Inc.),
L.R. Denham (Interactive Interpretation and Training, Inc.),
P.J. Desai (Geophysical Development Corp.),
M.E. Guthrie (Geophysical Development Corp.) &
M.A. Dunn (Geophysical Development Corp.)

Summary

- Regional analysis of a 5,716 Gulf of Mexico well log database
- Prediction of AVO response, as well as prediction of velocities
- Useful to geophysicists.
- Regional trends derived from depth profile plots of well sand / shale velocity histograms.
- Four major sub-regions were delineated, based on these profiles:
  1. Lower and Middle Miocene Shelf
  2. Upper Miocene through Pleistocene Shelf
  3. Upper to Middle Slope
  4. Lower Slope
- Strong velocity inversion is common in the geopressured Miocene in the deep Lower and Middle Miocene Shelf region.
- In the deep Upper Miocene through Pleistocene Shelf velocity inversion is less pronounced.
- The present deep water area shows a slower velocity increase with depth throughout the lithologic section than is seen on the shelf above geopressure, but has a much narrower range in spatial variation than is seen on overpressured rocks on the deep shelf.
- The Lower Slope appears to have a greater spread in sand and shale P-wave velocities than is seen in the Upper to Middle Slope areas.
- Allows prediction of the velocities which should be seen by the processing geophysicist.
- Velocity functions seen are those usually associated with multiple reflections, and as such, often discounted by the processor.

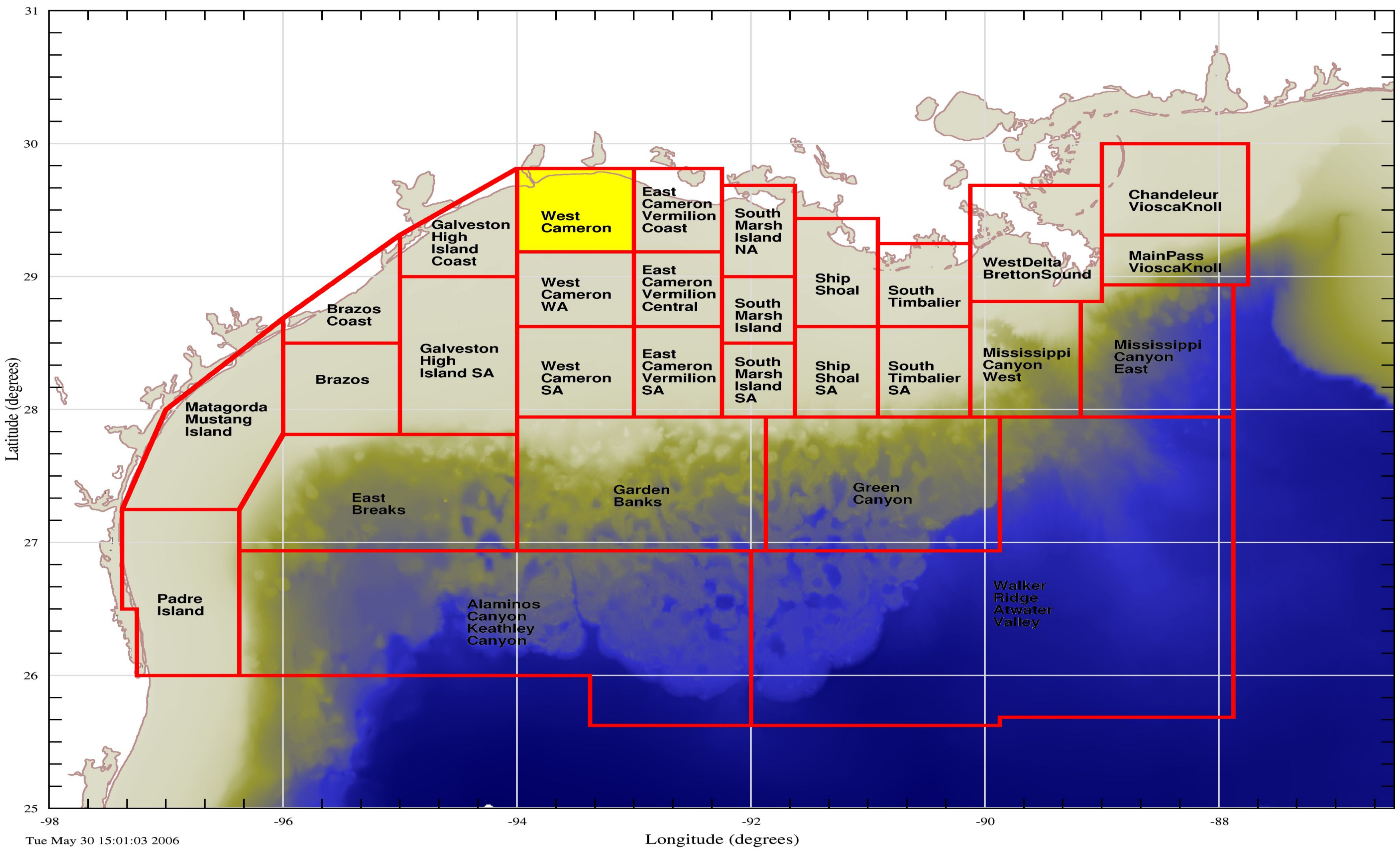

Figure 1: Tile Boundaries with the West Cameron Tile highlighted in yellow

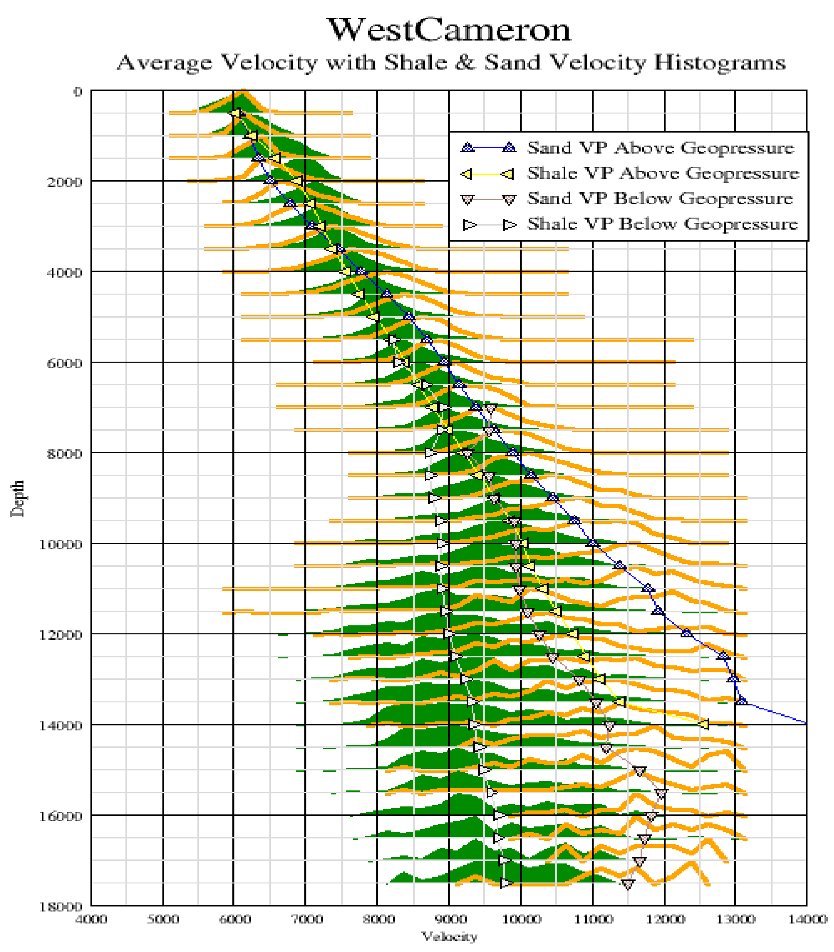

Figure 2: West Cameron Tile Shale and Sand Velocity Histogram

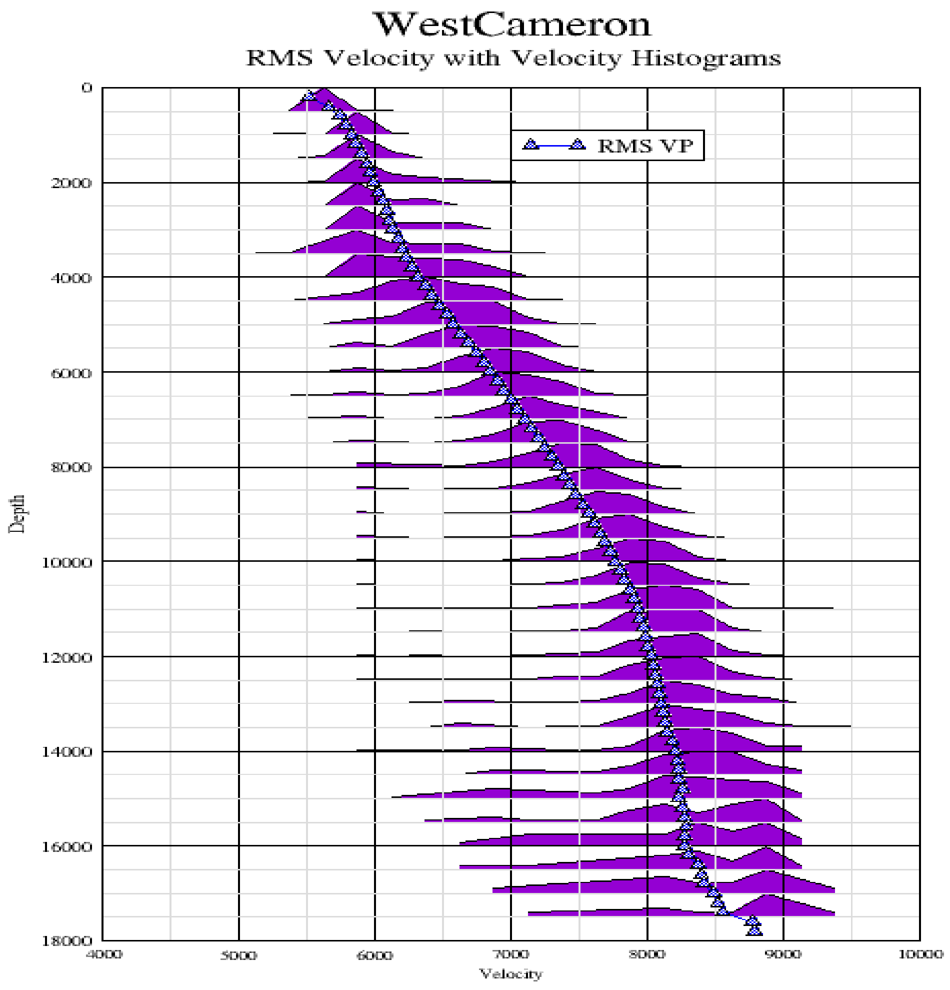

Figure 3: RMS velocity, West Cameron Tile

Introduction

AVO signatures in geopressured sections of siliciclastic basins vary greatly depending on the acoustic structure of these sediments. Especially important to gas and oil exploration in the deep shelf and deep water environments is an understanding of AVO Class distribution with depth and area. (Rutherford and Williams, 1989)

Data

The data for the study comprises well logs from 5,716 wells in the Gulf of Mexico waters, including the Texas and Louisiana shelf, continental slope, and deep water zones. Total depth ranges for these wells is from 340 meters to 9,046 meters, and water depth ranges from 1 meter to 2,995 meters. For most wells a suite of logs including sonic, density, resistivity, and SP curves are available, though in many cases some or all logs did not extend to the sea floor. All wells were digitized and loaded into a database. The data loading and quality control process extended over two decades. This same process can be applied to any basin where well logs are available.

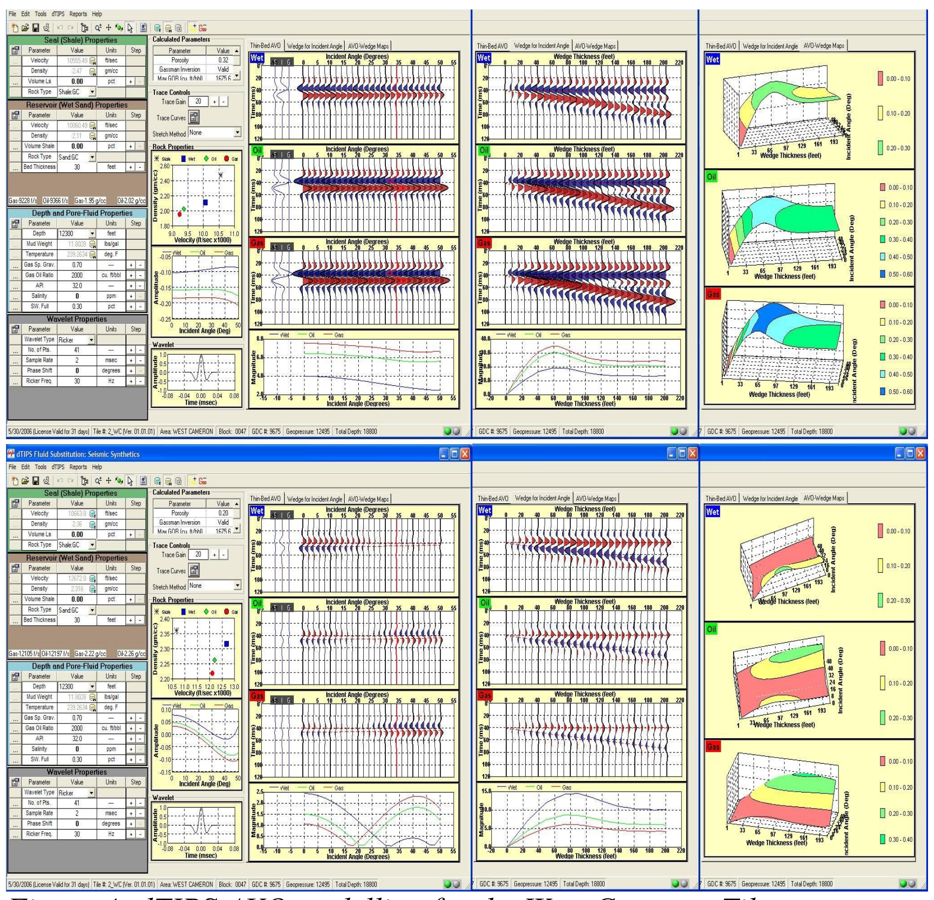

Figure 4: dTIPS AVO modelling for the West Cameron Tile

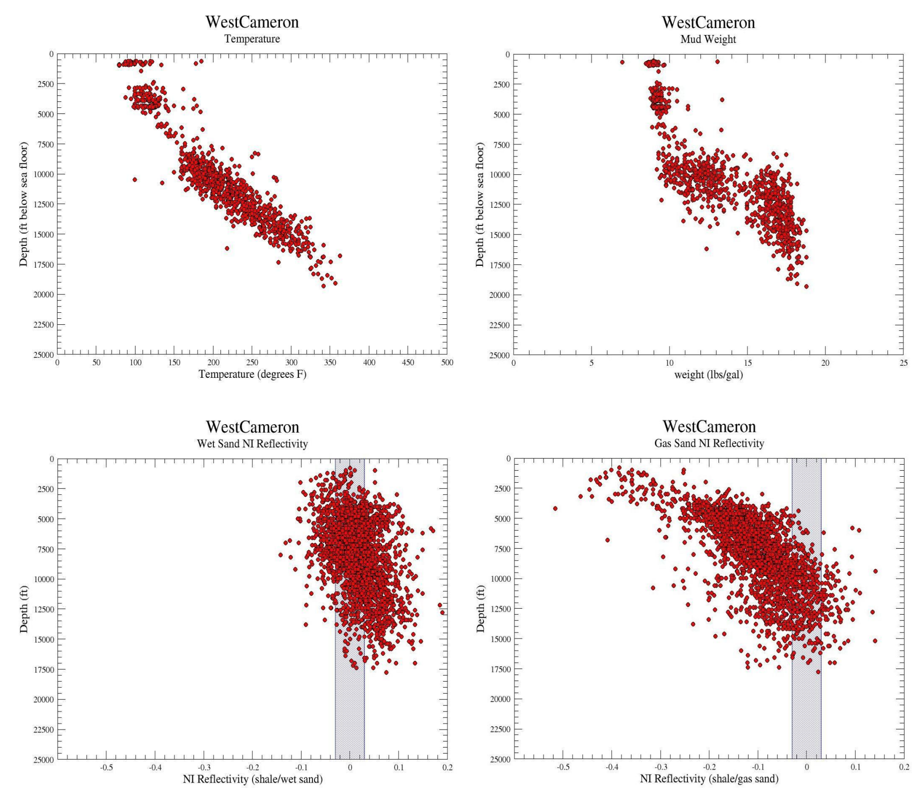

Figure 5: Temperature, Pressure, NIwet, and NIgas for the West Cameron Tile

Analysis

To balance the need for a statistically significant number of measurements against the desire to keep local variations, the Gulf of Mexico well log database was divided into areas, each called a Tile as shown in Figure 1. The Tiles in deeper water cover much larger areas, not because the geology is less variable, but because the number of available wells is much smaller. A Tile includes between 54 and 341 wells, and the wells have been selected so as to be distributed as evenly as possible across the Tile.

Because sands and shales behave differently with compaction, and since compaction is a function of time of burial as well as depth of burial, the first step was to create a lithology log, separating the dominantly sandy intervals of each log from the dominantly shale intervals using the gamma, SP, and neutron-density logs, as available for each well (Hilterman et al, 1998, Hilterman and Dunn, 2004). For this analysis, intervals with more than 50% sand were assigned to “sand”, and those with less than 50% sand were assigned to “shale”. Other lithologies were not considered. Hydrocarbon bearing sands were omitted from the analysis.

Separate average sand and shale velocities were computed over each 60 meter depth interval, using a sea-bottom datum. From the velocity measurements, mud weights, and other logs, the depth to the shallowest overpressured shale was identified in each well where possible. Over 3,400 wells encountered a transition from normal pressure to geopressure.

Within each tile, histograms and averages of sand and shale velocities were computed for each 150 meter interval (again, using the sea floor as a datum), separating normally-pressured and overpressured intervals for each lithology. For each Tile a composite plot was prepared to summarize the information, combining the sand and shale velocity histograms for the Tile with sand and shale velocities above and below the depth of the shallowest overpressured shale. The histograms are normalized to the maximum count within each depth interval.

Plotting depth profiles of well-derived sand and shale velocity histograms for each Tile illustrates changes across the region. Figure 2 shows a typical Tile summary plot, and is from the West Cameron Tile highlighted in Figure 1. The shale velocity histograms are shown in green, and the sand histograms are shown in yellow. Within this plot a clear separation between sand and shale velocities is seen on the shelf, and at greater depths the histograms are clearly bimodal. This plot summarizes velocity information from 321 wells. The depth scale is in feet and the velocity scale in feet per second.

To make the data more pertinent to seismic data processing, RMS velocities from sea level were computed for each well. As many of the wells did not have data extending to the sea floor, a velocity of 1,825 m/s was assumed from sea floor to the top of the logged interval. The resulting velocities were plotted similar to the sand and shale velocities, again on a Tile by Tile basis (Figure 3). This is the RMS of the average of all velocities,

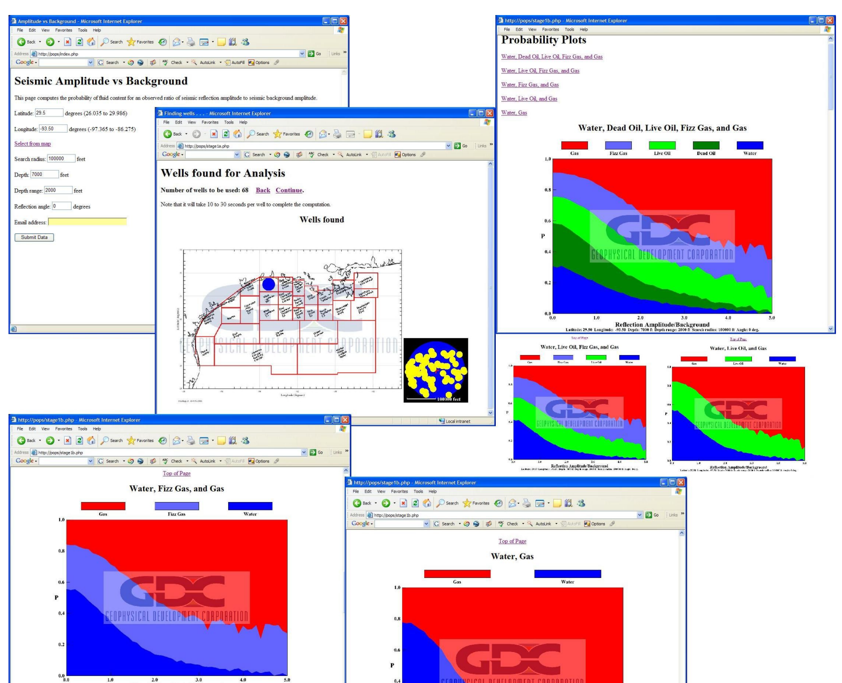

Figure 6: A/B Probability of Oil, Dead Oil, Fizz Gas, Gas, or Water for an Area Centered on the West Cameron Tile

computed for each 60 meter interval of each well, and referred to the sea level datum. The function of RMS velocity versus depth is similar to the plots of stacking velocity versus time widely used in seismic processing.

Software tools, including GDCMOD and d-TIPS, have been built to allow users to create or access an existing well log database. GDCMOD works with all available log curves at data collection sample rates. d-TIPS works with geophysical rock properties derived from the database at a user specified interval. Both software packages allow users to interactively model the AVO response. Figure 4 shows model results for a well in the center of the West Cameron Tile. Figure 5 shows pressure, temperature, NIwet (Normal Incidence Reflection Coefficient for water-filled sands), NIgas (Normal Incidence Reflection Coefficient for gas-filled sands) plotted against depth. These data were derived from the database. Figure 6 shows the results of a user specifying the area around a location and a search radius, the wells with valid data over the specified depth interval from the database, and then A/B (Amplitude/Background) plots for normally-incident reflections highlighting the probably of water, dead oil, oil, fizz gas, and/or gas being found in this area.

There are unexpected results, even when focusing on the single example of data from the West Cameron Tile. For example, the Sand Vp Above Geopressure curve is almost a straight line from the sea floor to the deepest values (about 14,000 feet or 4,270 meters). Normal compaction leads the interpreter to expect the rate of increase of velocity to decrease with depth. Putting the plots at the center of each Tile on a regional map shows the regional variations in velocity behavior. The shelf areas have the clearly bimodal velocities, showing the presence of both normally pressured and overpressured sediments in the same small geographical area. Deep water data tends to be mostly unimodal (Figures 7 and 8).

These velocity variations directly impact anticipated AVO response, as shown in Figure 9. Here cross-plots of NIgas vs Depth are colored to highlight Class III, Class II (+/-0.03 Normal Incidence gas [NIgas] Reflection Coefficient), and potential Class I AVO responses. Note how the depth to the top of Class II AVO varies across the Gulf of Mexico. Also note the thickness where both Class III and Class II are anticipated to be found, as defined on these plots. These regional trends provide context to exploration projects, showing an interpreter what type of response to look for within a specific exploration area.

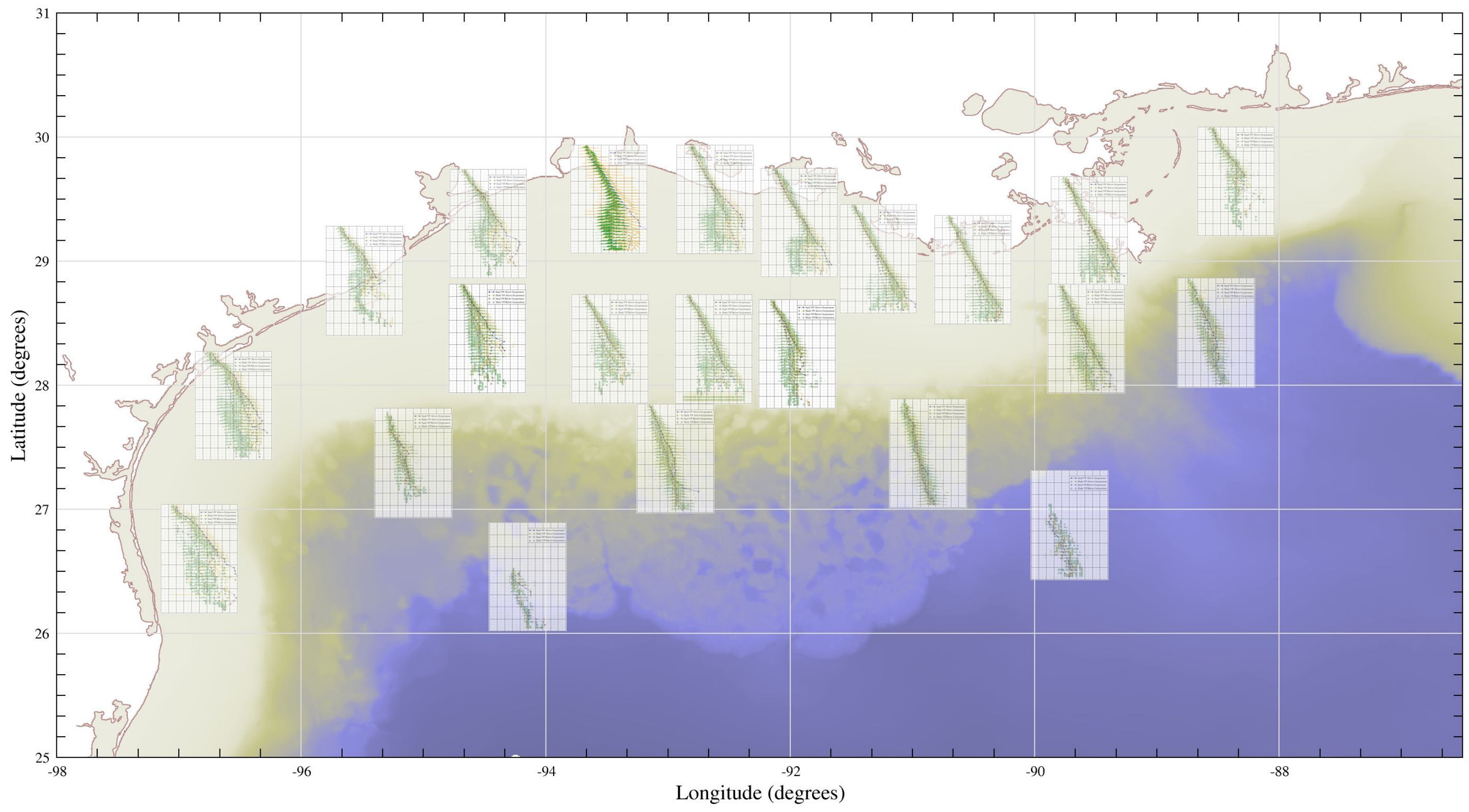

Figure 7: Variations in Sand/Shale Curves across the Gulf of Mexico

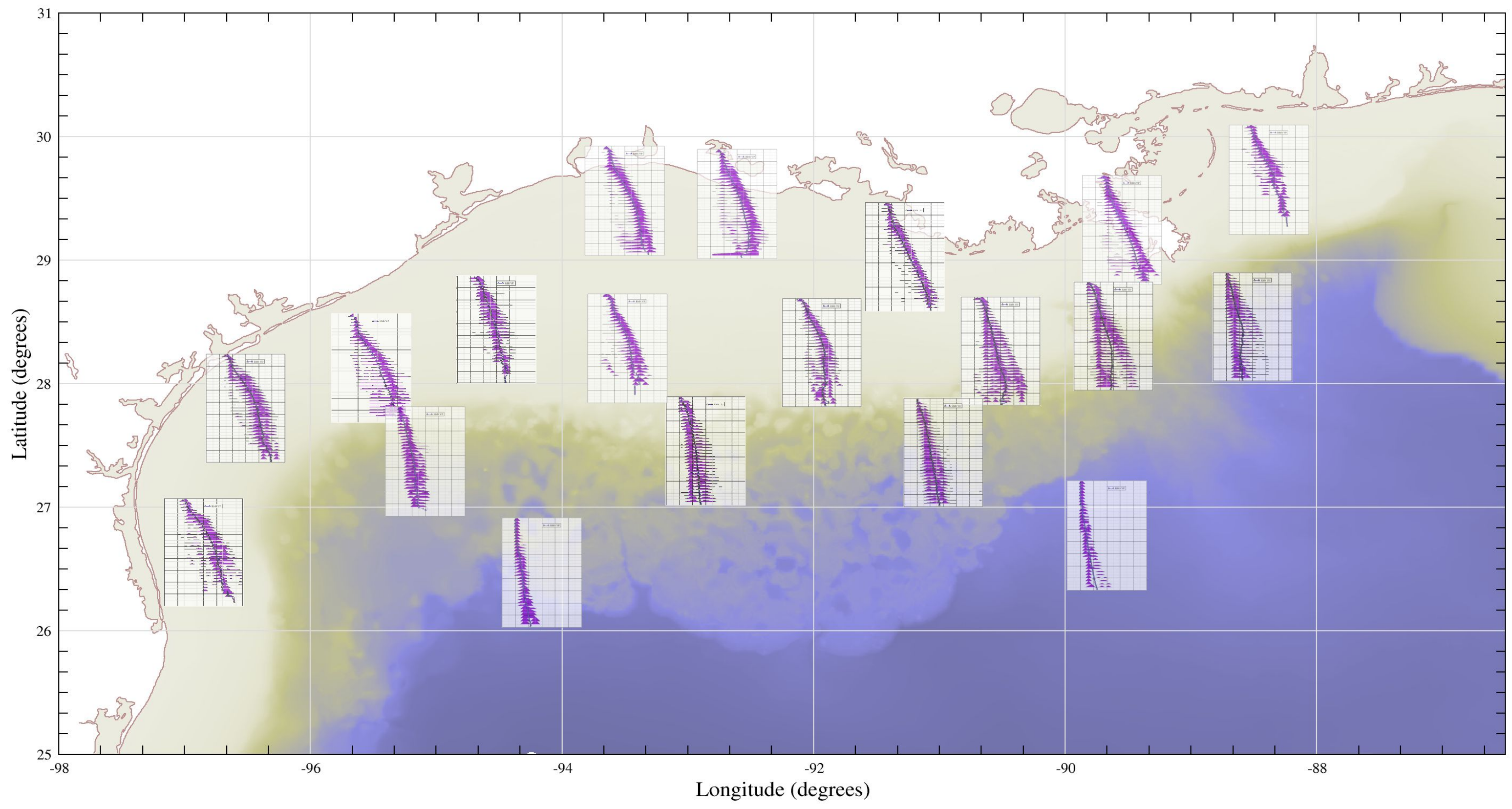

Figure 8: Variations in RMS Velocity Curves across the Gulf of Mexico

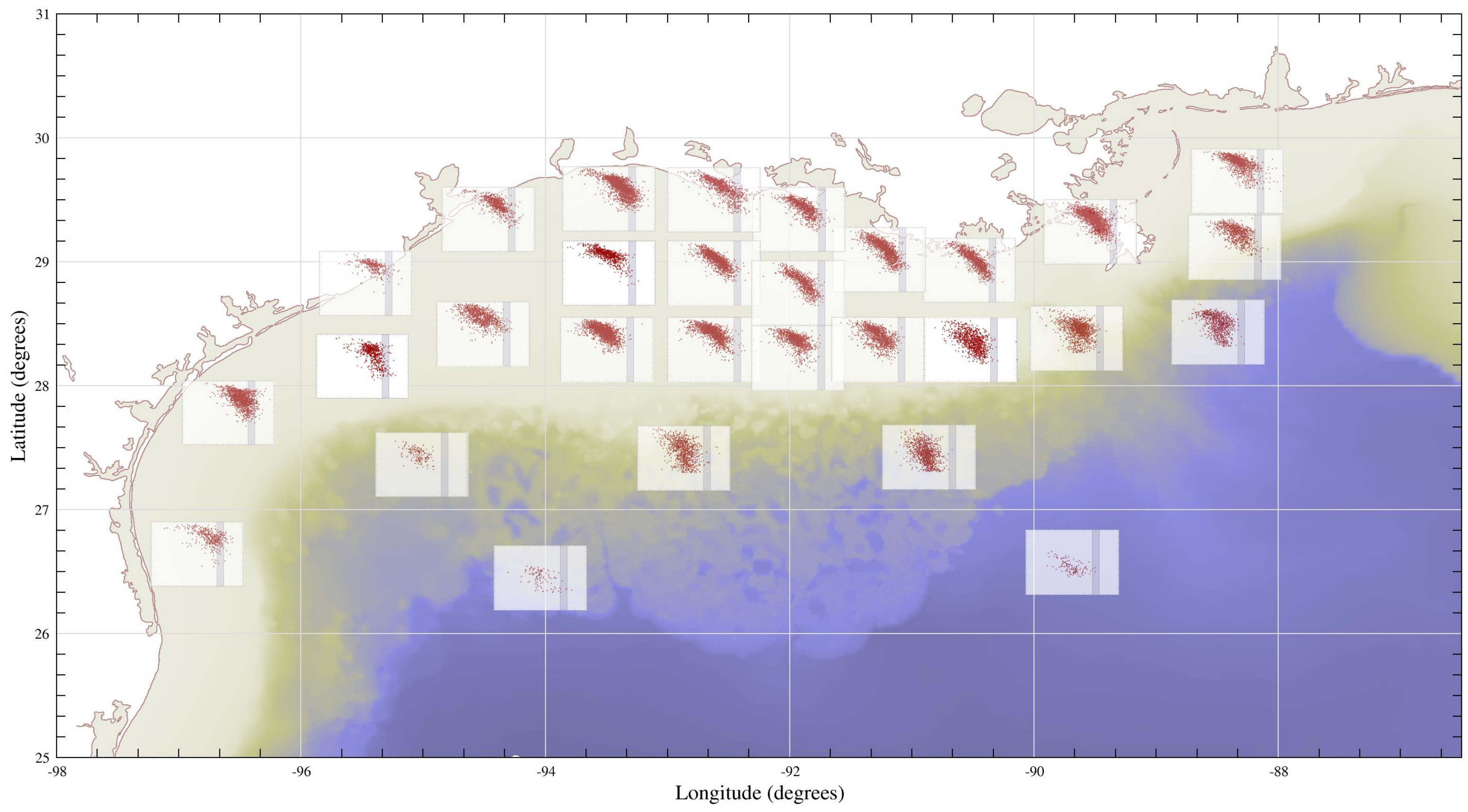

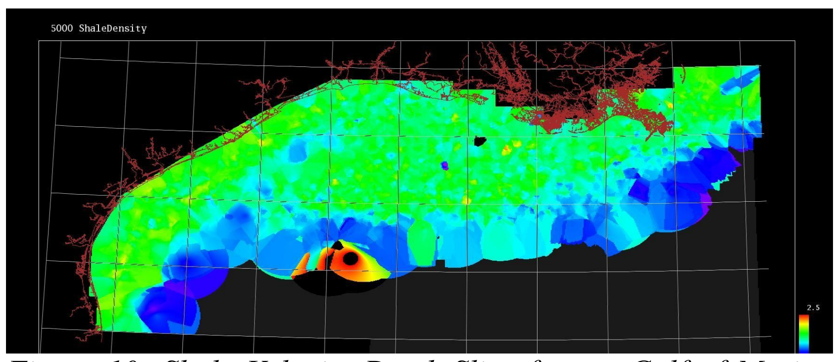
Figure 10: Shale Velocity Depth-Slice from a Gulf of Mexico SEG-Y Geophysical Rock Property Volume

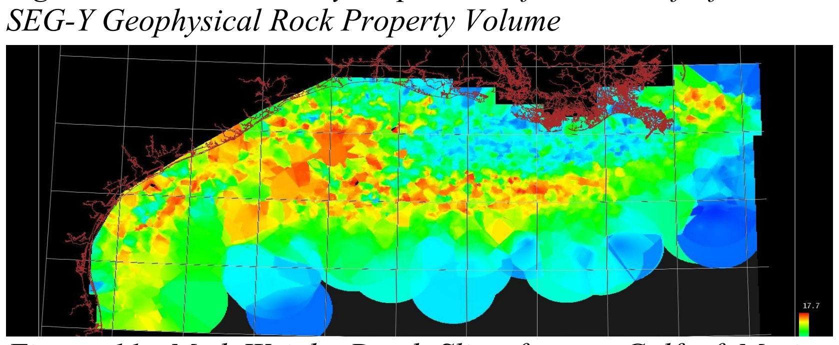
Figure 11: Mud Weight Depth-Slice from a Gulf of Mexico SEG-Y Geophysical Rock Property Volume

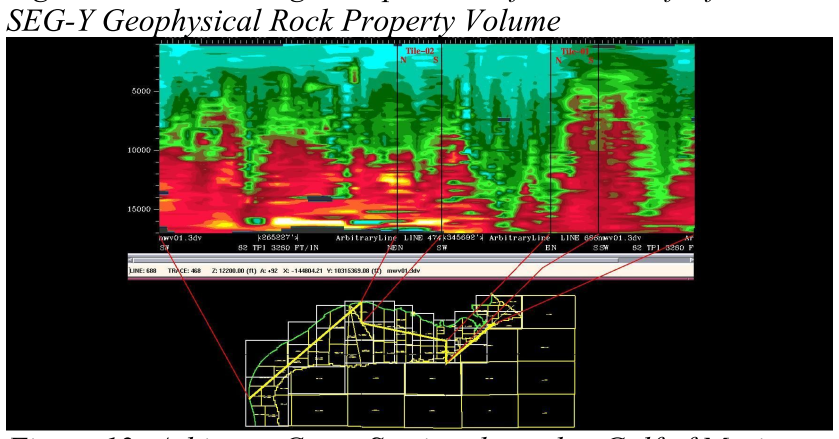
Figure 12: Arbitrary Cross-Section through a Gulf of Mexico Mud Weight SEG-Y Volume

To further enhance the interpreter's ability to integrate geophysical rock properties derived from well logs, software tools were built which allow a region (the entire Gulf of Mexico, a specific Tile, or bins that coincide with a pre-existing 3-D seismic survey) to be filled with SEG-Y traces of any of the 76 geophysical rock properties carried in a GDCMOD database. Figure 10 shows a depth slice at 1,524 meters, generated from a SEG-Y Shale Density volume. Figure 11 shows a depth slice at 3,048 meters, generated from a SEG-Y Mud Weight volume. Figure 12 shows a Landmark Graphics display of an arbitrary cross-section from a SEG-Y Mud Weight volume which goes through Tile-02 and Tile-01.

The extent of the interpreted four major sub-groups of seismic velocities across the region are shown in Figure 4. An obvious question which comes from this work is: Why is there such a difference in the velocities on the shelf and in deep water?

Conclusions

The strong velocity inversions seen in the deep Lower and Middle Miocene Shelf predict that geopressured gas reservoirs in this region will commonly generate Class II and even Class 1 AVO responses. The velocity structure in this area can also be expected to produce seismic processing difficulties, specifically in building stacking and migration velocity volumes. Inaccurate velocity estimates in the processing step can obscure even strong AVO gas signatures. As shown in Figure 5, there is considerable variation in AVO response at any depth.

Upper Miocene through Pleistocene Shelf geopressured reservoirs will also give Class II AVO responses. The less extreme transition to lithologic undercompaction associated with the onset of overpressure in this setting creates considerable overlap in the AVO Classes within any given depth interval.

Upper to Middle Slope profiles lack the extreme contrasts in AVO type seen on the shelf. Class III AVO responses are most common in this region, though Class II response is not uncommon. Portions of the area, for instance in Mississippi Canyon, have a more deep-shelf-like profile where Class II anomalies will be more common.

Observed Lower Slope sediments are similar to most Upper to Middle Slope profiles, but with a greater spread in rock properties. A wide range of AVO responses are expected to be interspersed in this region.

The RMS Velocities, prepared solely from well data, are effectively a simulation of an analysis tool used in seismic processing. They give the seismic processing geophysicist a method of evaluating the validity of a velocity model. Some of the wells clearly exhibit an RMS velocity which decreases with depth in the overpressured zones. Such decreases are widely considered to be an indication of multiples, and as such to be invalid for stacking or migrating seismic data. However, these results show such decreases to be real, based on analysis of individual wells and of large numbers of wells over a defined area.

Using results from this kind of well analysis will allow greater accuracy in determining the initial velocity model used for seismic data processing. The fewer iterations reduce the probability of using an erroneous model for expensive processes such as prestack depth migration, and will reduce processing time. Seismic data processed using such velocity models will allow a more reliable geological interpretation, and lower risk in drilling decisions. Perhaps the greatest advantage of the improved understanding of velocities will be with AVO analysis, which uses seismic data before it is stacked. Velocity errors prior to this analysis can have serious effects on the estimates of fluid content.

The importance of understanding these trends cannot be overstated when planning an exploration program in any siliciclastic basin. Although there is always variation from what is predicted, hydrocarbon exploration is a statistical business and proper understanding of the rock properties in a target area is key to increasing the explorer's probability of success.

This in turn depends on the P-wave velocity and the density response to sediment compaction trends.

Acknowledgements

The authors thank Geophysical Development Corporation for providing data for this paper.

References

Rutherford, S.R. and Williams, R.H. [1989] Amplitude-versus-offset in gas sands. Geophysics 54, 680-688.

Hilterman, F.J., Sherwood, J.W., Schellhorn, R., Bankhead, B. and DeVault, B. [1998] Identification of Lithology in the Gulf of Mexico. The Leading Edge 17(2), 215-222.

Hilterman, F.J. and Dunn, M.A. [2004] Identification of lithology in the Gulf of Mexico. 74th Meeting, Society of Exploration Geophysicists, Expanded Abstracts, 1710-1713.